

Ignition Delay for Jet Propellant 10/Air and Jet Propellant 10/High-Energy Density Fuel/Air Mixtures

David W. Mikolaitis,* Corin Segal,[†] and Abhilash Chandy[‡]
University of Florida, Gainesville, Florida 32611-6250

Jet propellant 10 [(JP-10) or exotetrahydrodicyclopentadiene] is one of the leading candidate fuels for use in pulse detonation engine applications. As such, its ignition delay characteristics have been studied previously in very dilute mixtures at pressures from 1 to 9 atm and temperatures from 1300 to 1670 K. The ignition delay times are studied of JP-10/air and JP-10 blended with methylated PCU alkene dimer, nitronorbornane, dinitronorbornane, and ethylhexylnitrate in air at pressures from 10 to 25 atm and temperatures from 1200 to 2500 K using a shock tube. Ignition delays were primarily measured using CH emission and secondarily using OH emission. Ignition delays were essentially insensitive to all of the additives tested. Additionally, ignition delays for dicyclopentadiene (a suspected intermediate in the combustion of JP-10) were also tested. Above 1500 K, multiple peaks in the CH emission were found. Further tests using OH emission indicate that the main peak in CH emission at these higher temperatures is probably due to reactions involved in the approach to equilibrium and give spuriously long ignition delay times.

Introduction

A PARTICULARLY attractive choice for a primary reference fuel for pulse detonation engine (PDE) applications is jet propellant 10 [(JP-10) or exotetrahydrodicyclopentadiene]. Recent work by Davidson et al.¹ has shed light on the ignition times for JP-10/O₂/Ar mixtures in the gas phase at low concentrations (0.2%) in the temperature range from 1350 to 1550 K at nominal pressures of 1.2 atm. Davidson et al.² extended the earlier work at a nominal pressure of 1 atm up to 1671 K and looked at pressures as high as a nominal 9 atm for temperatures up to 1400 K. In Refs. 1 and 2, peak values of CH emission are used to identify the time to ignition. Additional work completed at United Technologies Research Center³ cover the range 1300–1500 K and 3–7 atm. In Ref. 3, both pressure rise and peak OH emission are used to characterize the ignition delay. Our efforts are directed toward mixtures of JP-10 with high-energy density (HED) and other materials as sensitizers in air at higher temperatures and higher pressures such as would be encountered behind the leading shock in a detonation wave of a stoichiometric mixture JP-10 and air (possibly with fuel additives) in a PDE application.

The HED materials of interest here are with methylated PCU alkene dimer (MPCU) as shown schematically in Fig. 1, nitronorbornane, and dinitronorbornane synthesized by Marchand et al.^{4,5} Previous studies (Ref. 6, for example) have shown that HED additives can have substantial impact on the detonation properties of heavier hydrocarbon fuels. None of these materials have been specifically designed as a shock sensitizer for JP-10, and therefore, there is no guarantee that they will perform that task. Ethylhexylnitrate has also been suggested as a potential additive (Adroit Systems, personal communication).

Before we can proceed with the study of JP-10/HED blends we must first study JP-10/air mixtures and check the results for consistency with previous studies.

Experimental Setup

A double-diaphragm shock tube has been constructed at the University of Florida. The length of the driven section minus the test section length is 6.1 m and is made of 4-in. Schedule 80 seamless pipe, a commonly available pipe size for relatively high-pressure applications. The driver section is 1.8 m in length, also of 4-in. Schedule 80 seamless pipe. The test section is a stainless steel pipe 1.24 m long with a 3.5 cm i.d. and is added to the end of the main driven section. The test section is isolated from the main driven section by a 0.025-mm-thick Mylar[®] diaphragm. The smaller sized test section isolated from the main driven section is needed because only very small quantities of some of the HED fuels were available for testing. Both the test section and the main driven section can be evacuated with a vacuum pump, and they are normally are evacuated to the same pressure ranging from 0.2 to 0.3 atm depending on the anticipated shock strength and the desired final pressure. The liquid fuel is introduced with a calibrated syringe into a small stainless steel chamber adjacent to the test section and attached to the test section by stainless steel tubing. The fuel is then circulated through the test section for 15 min by an oilless pump to achieve a uniform mixture of known composition. The initial pressure in the test section is always sufficiently low to ensure full vaporization of the fuel mixtures. Our experience shows that 15 min is sufficient time to vaporize the liquid fuel fully. Near the end of the test section there is a PCB 113A26 high-speed pressure transducer, and at the end there is a 2.54-cm-diam, 12.5-mm-thick quartz window. Light emitted by the excitation of CH is detected by a Hamamatsu R374 photomultiplier after passing through a 430-nm filter with a ± 2 -nm bandwidth in an endwall configuration. Light emitted by OH emission can be detected by the same photomultiplier after passing through a 311-nm filter with a ± 4 -nm bandwidth. Two other PCB 113A26 high-speed pressure transducers are mounted in the main driven section, the second of which is very close to the end of the main driver section and right before the test section. Data from the high-speed pressure transducers and the photomultiplier tube are recorded with a National Instruments PCI-6110E data acquisition board at a sampling rate of 5 million samples per second on each data channel. This is the slowest device in the data acquisition and determines the temporal resolution of the experiment.

The shock speed can be calculated from the data recorded by three PCB 113A26 high-speed pressure transducers. The measured shock speed in the main driven section is always within 1% of the measured shock speed in the test section. The pressure transducer in the test section is located 9.5 mm upstream of the end of the tube, and the arrival of both the incident and the reflected shocks is clearly seen in the signal. The precise time of arrival of the shock at the end of

Received 18 June 2002; revision received 2 July 2002; accepted for publication 3 April 2003. Copyright © 2003 by the American Institute of Aeronautics and Astronautics, Inc. All rights reserved. Copies of this paper may be made for personal or internal use, on condition that the copier pay the \$10.00 per-copy fee to the Copyright Clearance Center, Inc., 222 Rosewood Drive, Danvers, MA 01923; include the code 0748-4658/03 \$10.00 in correspondence with the CCC.

*Associate Professor, Department of Mechanical and Aerospace Engineering, P.O. Box 116250; mollusk@ufl.edu.

[†]Associate Professor, Department of Mechanical and Aerospace Engineering, Associate Fellow AIAA.

[‡]Graduate Assistant, Department of Mechanical and Aerospace Engineering, Student Member AIAA.

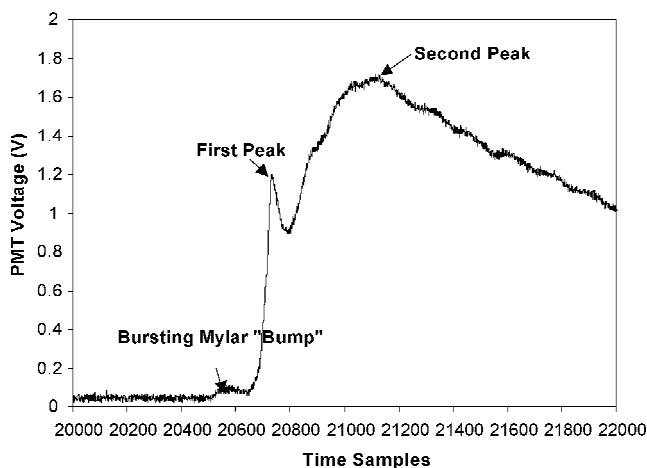
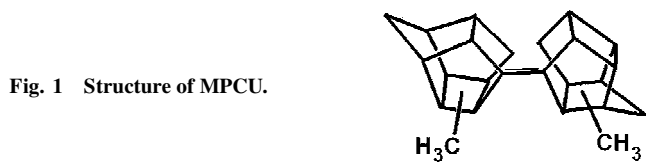


Fig. 2 Typical CH signal for intermediate temperatures.

the tube can be calculated from the knowledge of the incident shock speed. As a check, the reflected shock speed can be calculated, and the arrival time of the reflected shock can be predicted. It agrees with the measured time within the 0.2-ms resolution of the measurement.

At low temperature measurements, where a moderate amount of intensification is required, the light emissions from the bursting and possible weak reaction and melting of the Mylar diaphragm 1.24 m upstream of the detector can be detected as is shown in the example given in Fig. 2. This amount of light is small compared to the light emitted by the reaction of the fuel. Tests run without fuel at both high and low temperature confirms this. It is extremely unlikely that any reaction caused by the Mylar at the upstream end of the test section would have any influence on the reaction of the material of interest at the end of the test section.

Before each test, the test section is removed, cleaned with acetone, and air dried with compressed air. We have seen no effects of "seasoning" the test section after repeated tests or any effects that might be due to residual buildup on the test section walls.

Experimental Results: JP-10

Experiments run with JP-10/air mixtures without additives were run to validate the experimental procedure against previous work and to generate baseline data for tests with additives. The data from our experiments are shown in Tables 1 and 2.

At both the highest and the lowest temperatures studied here, there was only one peak in the CH emission, but for intermediate temperatures there are two peaks, as shown in Fig. 2 for a pressure of 15.8 atm and a temperature of 1495 K, with 0.2-ms time sample. We will refer to these as the first peak and the second peak.

At higher temperatures, the first peak becomes smaller relative to the second peak. An example is shown in Fig. 3, for a pressure of 19.0 atm and a temperature of 1680 K, with 0.2-ms time sample. At even higher temperatures, the first peak becomes undetectable, and only the broad second peak is found.

For lower temperatures, the first peak becomes considerably more pronounced relative to the second peak, as shown in Fig. 4 where only one peak is discernible. Here the temperature is 1234 K and the pressure is 12.9 atm, with 0.2-ms time sample. This signal looks very similar to the type of CH emission signal reported in Refs. 1 and 2. It is clear that the sole remaining peak shown in Fig. 4 is related to the first peak in Fig. 1 when the tests run at intermediate conditions are viewed.

Table 1 Stoichiometric JP-10/air ignition delay data: CH emission

Temperature, K	Pressure, atm	Peak 1 ignition delay, ms	Peak 2 ignition delay, ms
1231	11.4	415.1	
1234	12.9	573.7	
1269	12.0	377.7	
1317	9.6	309.4	
1374	15.5	228.7	
1407	10.7	206.7	
1495	15.8	56.2	134.9
1517	16.2	47.7	138.2
1680	19.0	37.7	129.7
1690	19.1	37.8	134.8
1835	16.3	9.3	126.3
1913	23.1	5.7	130.5
1913	23.1	7.1	129.5
1945	17.7	5.2	118.0
1962	24.0	5.7	128.7
2103	29.8		123.1
2368	23.5		117.1
2414	24.1		110.8
2434	24.4		102.8

Table 2 Stoichiometric JP-10/air ignition delay data: OH emission

Temperature, K	Pressure, atm	Peak 1 ignition delay, ms
1787	15.6	14.5
2006	18.6	11.4
2007	18.6	10.4
1840	24.5	6.7
1749	20.2	100.4
2140	20.4	10.6
1286	9.2	334.0
1167	7.8	2114.0
1313	9.6	316.0
1529	12.3	14.5
1651	18.5	9.6
1577	19.3	15.9
1303	12.6	294.7

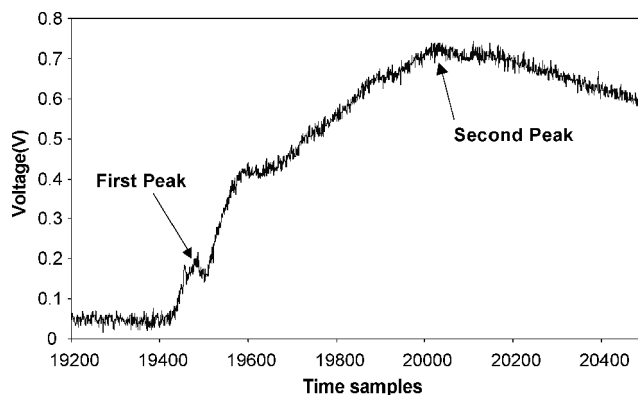


Fig. 3 Typical CH signal for high temperatures.

A plot of the raw data is shown in Fig. 5. The United Technologies Research Center (UTRC) data³ and the data from Davidson et al.,² here referred to as the Stanford data, are shown along with the data collected in this study. Only nominally stoichiometric results are shown. There are several important differences between these studies. First, the mixtures studied in Refs. 1–3 are greatly diluted with argon, whereas the mixtures studied here are stoichiometric JP-10/air mixtures. One would expect that the JP-10/air mixtures would have a shorter ignition time. Second, the data collected in this study are at a much higher pressure. In Ref. 2, it was seen that the ignition time decreased with increasing pressure, as would be expected. Both

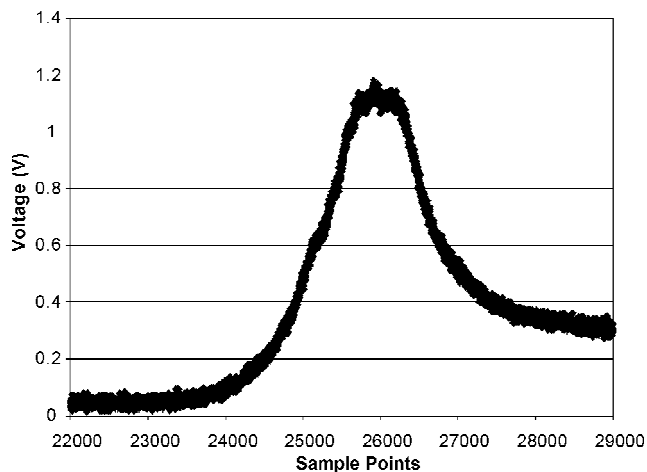


Fig. 4 Typical CH signal for low temperatures.

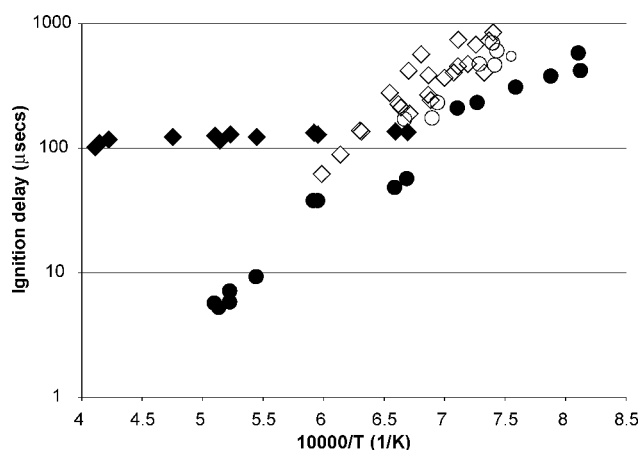


Fig. 5 Ignition delay vs temperature for JP-10, no pressure correction: ●, current study first peaks; ◆, current study second peaks; ○, UTRC data; and ◇, Stanford data.

of these effects point toward the anticipated ignition times in this study being shorter than those found in the earlier studies.

The data in Fig. 5 are consistent with this picture and with the earlier data only if the first peak in CH emission is considered. If an expression of the form $\tau = A \cdot P^n \cdot \exp(B/T)$ is used to correlate the data (where P is in atmospheres and T in Kelvin) and only the stoichiometric data is used, we have $n = -0.526$, and $B = 24,720$ K with an R^2 correlation of 0.943 for the Stanford data; $n = 0.04$, $B = 16,930$ K, and $R^2 = 0.892$ for the UTRC data; and $n = -0.162$, $B = 14,910$ K and $R^2 = 0.970$ in the present study. Ryan et al.,⁷ using a constant volume bomb in the pressure range of 25–30 atm and a temperature range of 590–855 K, report results with B in the range of 11,000–12,000 K. Stanford data and current data are given in Fig. 6.

Applying the preceding pressure correlations gives the result shown in Fig. 7. Here we see that there is a substantial difference in temperature dependence at these higher pressures. This is not obvious without applying the pressure correction. The results of this study are similar to those found in the high-pressure study by Ryan et al.⁷

The behavior at higher temperatures, where the second peak becomes dominant, is not seen in the earlier studies at lower pressures and temperatures. That the time to the second peak is nearly independent of temperature suggests that the rate limiting step is a recombination reaction. This suggests that the second peak might be due to a recombination reaction on the approach to equilibrium. This can be tested by looking at OH emission as well. In Fig. 8 we show a series of tests using JP-10/air mixtures where CH and OH emissions are used to determine ignition times. In this case, the first peak in OH stays dominant even to elevated temperatures.

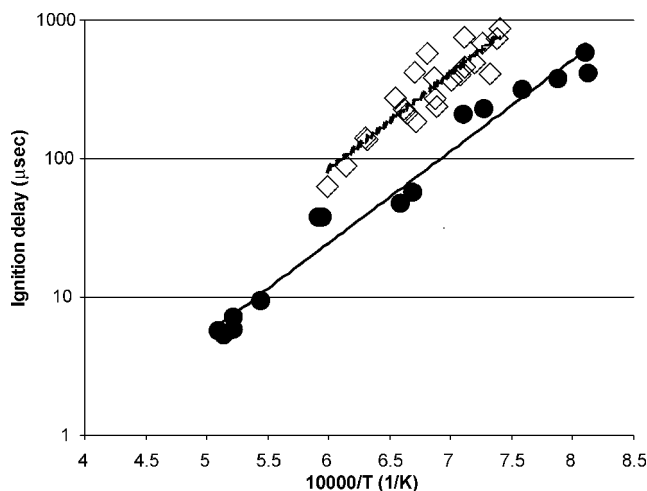


Fig. 6 Ignition delay vs temperature for stoichiometric JP-10 mixtures: ◇, Stanford data (JP-10/O₂/argon); ●, current study (JP-10/air); and —, least-squares curve fits to the data.

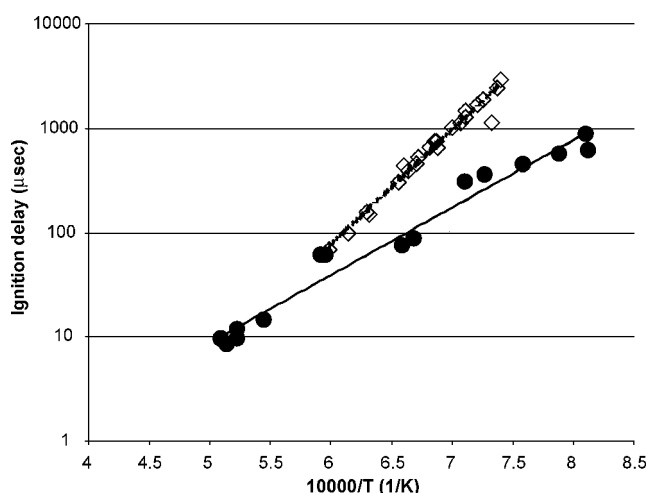


Fig. 7 Pressure-corrected ignition times for stoichiometric JP-10 mixtures: ◇, Stanford data (JP-10/O₂/argon); ●, current study (JP-10/air); and —, least-squares curve fits to the data.

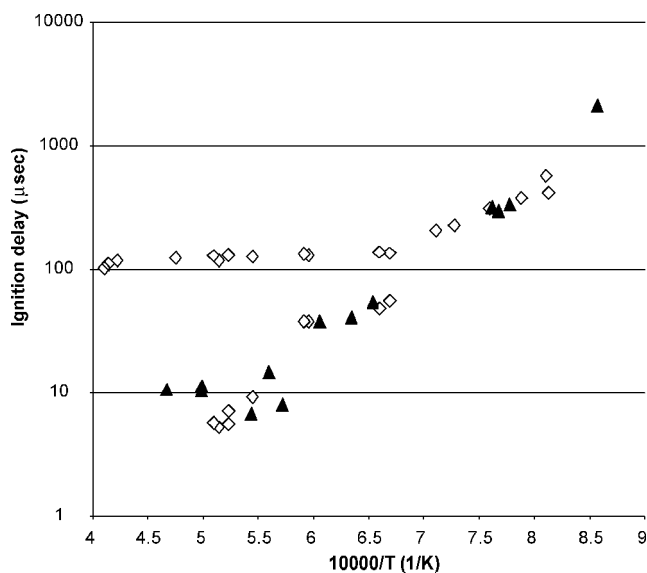


Fig. 8 Measured ignition delays for stoichiometric JP-10/air mixtures: ◇, CH emission and ▲, OH emission.

This indicates that even though the first peak in CH emission can be quite small relative to the second peak, it is the true indicator of ignition. Note that, when conditions behind the reflected shock were near the extrapolation of the second explosion limit, the OH emission signal appeared to "ring." We attribute this to weak expansion waves generated by the reaction reflecting off the endwall as compression waves and then perturbing the local pressure where reaction is occurring. These small variations in pressure can cause major changes in OH production because of the proximity of the second explosion limit. If the data for OH from the present study is used, then $n = -1.36$ and $B = 9800$ K with $R^2 = 0.795$, showing a much stronger pressure dependence and a much lower activation energy than the CH emission data indicate.

No attempt was made to control the amount of water vapor in the air or from outgassing from the test section walls. Only at the lowest temperatures studied, where other researchers have already supplied data, would we expect that the high third-body efficiency of water in the hydrogen/oxygen chain-breaking reaction $H + O_2 + M \rightarrow HO_2 + M$ to play an important role. For this, reason it was thought that control of water vapor concentrations would not be critical.

Experimental Results: JP-10 with Additives

MPCU was designed as an HED fuel, not specifically as an additive to lower ignition delays in shock initiated combustion.⁴ It does have some features that make it attractive as a fuel additive in PDE applications, however. MPCU has shown itself to be capable of increasing deflagration speeds of JP-10 by a factor of five (Ref. 8) and undoubtedly can increase Chapman–Jouguet detonation wave speeds due to its enormous energy density. On the other hand, one would expect that MPCU has very large activation energy, and this would tend to increase the ignition delay.

In Fig. 9, the results of a series of shock tube measurements for JP-10 with and without the addition of MPCU are shown. The experimental data are also shown in Table 3. On the face of it, this shows little difference in ignition delay times as compared to pure JP-10. Note, however, that the intensity levels for the CH emissions were reduced substantially and that there was a broad peak in CH emission much later, typically around 4 ms after the shock arrival. Our interpretation of these results is that there is little interaction between the ignition of the JP-10 and MPCU and that the MPCU ignites much later due to its very large activation energy. We do not present the time to reach the MPCU ignition peak because it is beyond the time by which a shock reflected off the contact surface would reach the end of the test section. The ignition delays are so large as to make MPCU a poor choice as an additive to JP-10 for PDE applications. The data for stoichiometric 90% JP-10/10% MPCU mixtures in air correlated with $\tau = 9.4 \times 10^{-12} s \times P^{0.962} \times \exp(19,780 \text{ K}/T)$,

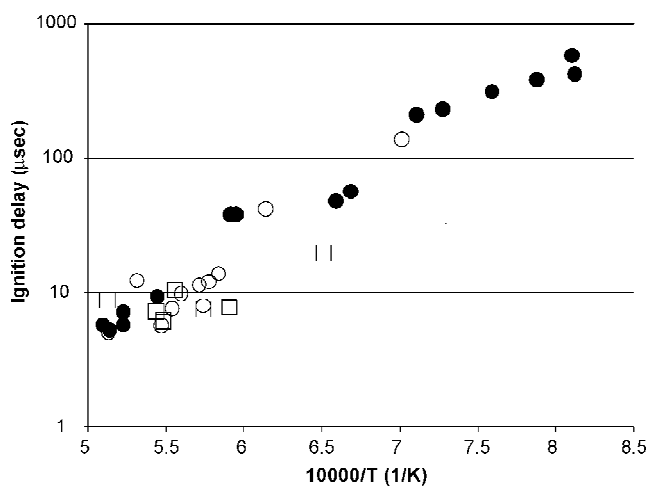


Fig. 9 Ignition delay for stoichiometric JP-10/MPCU blends in air: ●, JP-10; ○, 10% MPCU; and □, 50% MPCU.

Table 3 Stoichiometric JP-10/MPCU/air ignition delay data: CH emission

Temperature, K	Pressure, atm	Peak 1 ignition delay, ms	Peak 2 ignition delay, ms
<i>Stoichiometric JP-10/10% MPCU/air</i>			
1426	14.6	136	191.2
1628	18.1	41.5	127.1
1712	14.7	13.7	121.3
1731	17.4	11.9	134.9
1741	15	8	129.6
1749	15.1	11.2	138
1785	20.8	9.7	116.7
1805	21.2	7.6	121.6
1827	21.6	5.7	126.1
1881	22.5	12.2	122.6
1948	17.8	5	118
2015	18.7		112.8
2213	21.4		98.4
<i>Stoichiometric JP-10/50% MPCU/air</i>			
1416	14.4	217.8	
1421	16.3	193.8	
1536	16.5	19.6	132.9
1693	21.6	7.8	166.6
1743	22.6	7.6	146.6
1800	21.1	10.4	141.8
1824	21.5	6	128.2
1824	21.5	6.2	128
1840	16.3	7.3	158.3
1952	26.7	8.9	336.7
2014	18.7		121.8
2105	19.9		119.9
1498	11.9		148.6
1588	13		146.6
1822	16.1		120.6

Table 4 Stoichiometric JP-10/ethyl-hexyl nitrate/air ignition delay data: CH emission

Temperature, K	Pressure, atm	Peak 1 ignition delay, ms	Peak 2 ignition delay, ms
1158	10.2	1388	
1348	10.0	193	211
1394	10.6	132	163
1476	15.5	60	117.5
1712	14.6	17.1	142
1749	22.7	11.4	128
1897	25.6	13.3	125
1996	24.6	12.0	126
2051	19.2	12.1	128

Table 5 Stoichiometric JP-10/nitronorbornane/air ignition delay data: CH emission

Temperature, K	Pressure, atm	Peak 1 ignition delay, ms	Peak 2 ignition delay, ms
2114	20		140.5
1983	24.3		150.1
1855	24.8		136
1771	15.4	12.7	138.9
1747	15.1		140.4
1714	19.6		149.9
1497	17.8	19	131.4
1486	11.7	22.5	137.7

$R^2 = 0.893$, with P in atmospheres. The correlation for 50% MPCU is $\tau = 2.0 \times 10^{-10} s \times P^{0.106} \times \exp(18,480 \text{ K}/T)$, and $R^2 = 0.838$.

In Fig. 10, we show the ignition time results for most of the other additives. Again we see very little impact on ignition time and the same trend showing multiple peaks at higher temperatures. Numerical values are found in Tables 4–6. The data with ethyl-hexyl nitrate as the additive yielded $n = -0.17$ and $B = 12,470$ K with $R^2 = 0.947$ and the data for dinitronorbornane as the additive

Table 6 Stoichiometric JP-10/20% dinitronorbornane/air ignition delay data: CH emission

Temperature, K	Pressure, atm	Peak 1 ignition delay, ms	Peak 2 ignition delay, ms
2165	20.7	11.4	126.6
2020	25.0	8.0	164.2
1643	13.8	17.0	148.0
1862	16.6	7.4	143.0
1365	10.2	211.7	

Table 7 Stoichiometric dicyclopentadiene/air ignition delay data: CH emission

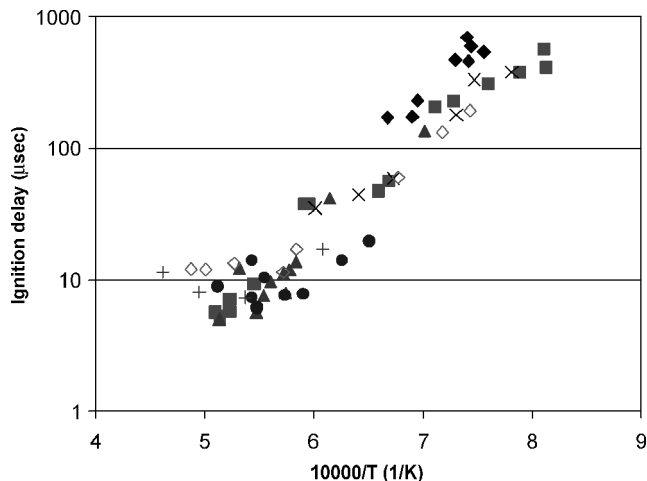
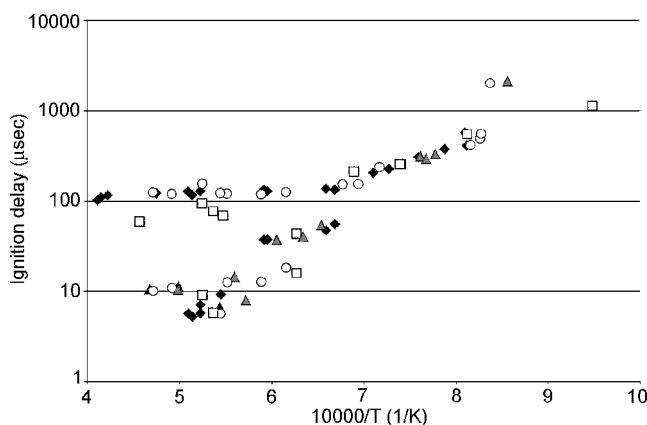
Temperature, K	Pressure, atm	Peak 1 ignition delay, ms	Peak 2 ignition delay, ms
1904	22.9	156.7	
1699	14.5	12.8	119.8
1394	10.6	238.6	
2121	20.1	10.1	125.1
1837	24.4	5.7	123.5
1440	14.9	155.3	
1624	15.7	18.3	126.7
1476	17.4	154.3	
1209	12.4	494.5	
1225	11.3	419.4	
1193	8.1	2002.6	
2033	18.9	10.9	120.9
1812	16	12.6	122.2
1208	12.4	556.3	

Table 8 Stoichiometric dicyclopentadiene/air ignition delay data: OH emission

Temperature, K	Pressure, atm	Peak 1 ignition delay, ms	Peak 2 ignition delay, ms
1905	17.2	9.1	94.5
1450	11.3	212.7	
2188	21	59.7	
1595	19.7	16	43.8
1863	22.2	5.8	77.8
1827	24.2	69.7	
1351	13.4	257	
1352	15.1	257.6	
1230	11.4	552.1	
1054	8.6	1125.1	

yielded $n = 0.361$ and $B = 12,740$ K with $R^2 = 0.813$. Because there are only three data points with first peaks for CH for nitronorbornane as the additive, we find little value in fitting the data.

In Fig. 11, we show a series of tests using JP-10 and dicyclopentadiene/air mixtures where CH and OH emissions are used to determine ignition times. Numerical values are shown in Tables 7 and 8. In this case, the first peak in OH stays dominant even to elevated temperatures for JP 10. The second peaks in OH emission for the dicyclopentadiene/air mixtures occur and swamp out the first peak for temperatures greater than 1830 K or so. These tests were made because dicyclopentadiene is a likely intermediary in the reaction of JP-10 in air and it also contains pentagonal carbon structures. The similarity in ignition results suggests that similar rate controlling reactions occur in both systems. The differences for behavior after the first peak is most likely due to different paths to equilibrium caused by different ratios of hydrogen to carbon in the two fuels. The ignition delay data using peak CH yields $\tau = 2.5 \times 10^{-8} s \times P^{-0.044} \times \exp(12,450 \text{ K}/T)$, and $R^2 = 0.774$, and using peak OH gives $\tau = 8.3 \times 10^{-5} s \times P^{-1.55} \times \exp(6545 \text{ K}/T)$, and $R^2 = 0.699$. Again we see the stronger pressure dependence and lower activation energy when OH peak is used for defining the ignition delay ($n = -1.36$ and $B = 9800$ K with $R^2 = 0.795$ for stoichiometric JP-10/air).

**Fig. 10** Ignition delays for stoichiometric JP-10/additive blends in air: ♦, UTRC JP-10 data; ■, current study JP-10 data; ▲, 10% MPCU; ●, 50% MPCU; ×, 10% nitronorbornane; +, 20% dinitronorbornane; and ◇, 10% ethyl-hexyl nitrate.**Fig. 11** Ignition delays for stoichiometric JP-10/air and dicyclopentadiene/air using CH and OH emissions: ♦, JP-10/air with CH emission; ▲, JP-10/air with OH emission; ○, dicyclopentadiene/air with CH emission; and □, dicyclopentadiene/air with OH emission.

Conclusions

Ignition delays for JP-10/air and JP-10/additive blends in air have been experimentally determined for temperatures from 1200 to 2500 K and for pressures from 10 to 30 atm. CH emission showed multiple peaks at temperatures higher than 1500 K. A series of tests run with JP-10/air mixtures where OH emission was detected only showed a single dominant peak occurring at a time similar to the first peak in the CH emission. At very high temperatures, the first CH peak was not detected because its signal was weak compared to the second peak. This second peak in CH emission is probably due to a recombination reaction during the approach to equilibrium, so that using CH emission in that regime is not suitable for determining ignition delays. Using OH emission for determining ignition delay times for the high-temperature and pressure tests was effective, but the correlations were different from the correlations using CH emission (much stronger pressure dependence and much smaller activation energy).

It was found that none of the additives studied (methylated PCU alkene dimer, nitronorbornane, dinitronorbornane, and ethyl-hexyl nitrate) lowered ignition delays of JP-10 to any appreciable degree in the temperature and pressure range studied, and therefore, none of these should be used for that purpose.

Ignition behavior of JP-10 and dicyclopentadiene/air mixtures shows very similar behavior, suggesting that the rate controlling kinetics in each case is similar. The ignition delays were similar for both the peak CH emission and for the peak OH emission.

Acknowledgments

We would like to acknowledge that this work was performed under the Office of Naval Research Contract N00014-99-1-0745 and was monitored by Gabriel Roy.

References

- ¹Davidson, D. F., Horning, D. C., and Hanson, R. K., "Shock Tube Ignition Time Measurements for N-Heptane/O₂/Ar and JP-10/O₂/Ar Mixtures," AIAA Paper 99-2216, June 1999.
- ²Davidson, D. F., Horning, D. C., Herbon, J. T., and Hanson, R. K., "Shock Tube Measurements of JP-10 Ignition," *Proceedings of the Combustion Institute*, Vol. 28, 2000, pp. 1687–1692.
- ³Colket, M. B., III, and Spadaccini, L. J., "Scramjet Fuel Autoignition Study," *Journal of Propulsion and Power*, Vol. 17, No. 2, 2001, pp. 315–323.
- ⁴Marchand, A. P., Namboothiri, I., Sulejman, A., Kumar, K., Lewis, S., "Large Scale Synthesis of New High Energy/High Density Hydrocarbon Fuel Systems," *Proceedings of the 11th ONR Propulsion Meeting*, Naval Research, Arlington, VA, 1998, pp. 87–94.
- ⁵Marchand, A. P., Zope, A., Zaragoza, F., Bott, S. G., Ammon, H. L., and Du, Z., "Synthesis, Characterization and Crystal Density Modeling of Four C₂₂H₂₄ Cage Functionalized Alkenes," *Tetrahedron*, Vol. 50, No. 6, 1994, pp. 1687–1698.
- ⁶Ranger, A. A., and Nicholls, J. A., "Aerodynamic Shattering of Liquid Drops," *AIAA Journal*, Vol. 7, No. 2, 1969, pp. 285–290.
- ⁷Ryan, T. W., Schwab, S. T., and Harlow, W. W., "Aluminum Alkyl Derivatives: Ignition and Combustion Enhancers for Supersonic Combustors," *Journal of Propulsion and Power*, Vol. 11, No. 1, 1995, pp. 124–129.
- ⁸Segal, C., Pethe, S., and Williams, K. R., "Combustion of High-Energy-High-Density Fuels," *Combustion Science and Technology*, Vol. 163, No. 2, Feb. 2001, pp. 229–244.